CAMBRIDGE
UNIVERSITY PRESS

Article

Argentotetrahedrite-(Cd), Ag$_6$(Cu$_4$Cd$_2$)Sb$_4$S$_{13}$, a new member of the tetrahedrite group from Rudno nad Hronom, Slovakia.

Tomáš Mikuš[1]*, Jozef Vlasáč[1], Juraj Majzlan[2] (iD), Jiří Sejkora[3] (iD), Gwladys Steciuk[4], Jakub Plášil[4] (iD), Christiane Rößler[5] and Christian Matthes[5]

[1]Earth Science Institute, Slovak Academy of Sciences, Ďumbierska 1, 974 11 Banská Bystrica, Slovakia; [2]Institute of Geosciences, Friedrich-Schiller University, Burgweg 11, 07749 Jena, Germany; [3]Department of Mineralogy and Petrology, National Museum, Cirkusová 1740, 193 00 Praha 9, Czech Republic; [4] Institute of Physics ASCR, v.v.i., Na Slovance 1999/2, 18221 Praha 8, Czech Republic; and [5]Bauhaus University, Coudraystrasse 11, 99423 Weimar, Germany

Abstract

Argentotetrahedrite-(Cd), Ag$_6$(Cu$_4$Cd$_2$)Sb$_4$S$_{13}$, has been approved as a new mineral species by the Commission on New Minerals, Nomenclature and Classification of the International Mineralogical Association using samples from Rudno nad Hronom, Slovak Republic. It occurs as anhedral grains up to 30 μm in size, steel-grey to black in colour, with a metallic lustre, in association with green-ockite and other tetrahedrite-group minerals [argentotetrahedrite-(Zn) and tetrahedrite-(Zn)], earlier base-metal minerals, Ag sulfides and sulfosalts (acanthite, pyrargyrite and polybasite) and later galena. Argentotetrahedrite-(Cd) is isotropic, grey in colour, with a creamy tint and rapidly (tens of minutes) tarnishes to orange–brown. Reflectance data for Commission on Ore Mineralogy (COM) wavelengths in air are [λ (nm), R (%)]: 470, 30.4; 546, 30.3; 589, 30.3; and 650, 28.7. The chemical formula of the samples studied, recalculated on the basis of $\Sigma Me = 16$ atoms per formula unit, is: (Ag$_{3.28}$Cu$_{2.72}$)$_{\Sigma6.00}$[Cu$_4$(Cd$_{1.68}$Fe$_{0.27}$Zn$_{0.16}$)]$_{\Sigma6.11}$(Sb$_{3.71}$As$_{0.15}$)$_{\Sigma3.86}$S$_{12.79}$. Argentotetrahedrite-(Cd) is cubic, $I\bar{4}3m$, with $a = 10.65(2)$ Å, $V = 1208(4)$ Å^3 and $Z = 2$. Argentotetrahedrite-(Cd) is isotypic with other members of the tetrahedrite group. The structural relationship between argentotetrahedrite-(Cd) and other members of the freibergite series are discussed and previous findings of this species are briefly reviewed.

Keywords: tetrahedrite group, argentotetrahedrite-(Cd), new mineral, sulfosalt, copper, silver, antimony, cadmium, crystal structure

Introduction

Tetrahedrite-group minerals are the most common sulfosalts in many hydrothermal ore deposits. These chalcogenides form a complex isotypic series, with the general structural formula $^{M(2)}$A$_6$$^{M(1)}$(B$_4C_2$)$^{X(3)}D_4$$^{S(1)}Y_{12}$$^{S(2)}$Z, where A = Cu$^+$, Ag$^+$, □ (vacancy) and (Ag$_6$)$^{4+}$ cluster; B = Cu$^+$ and Ag$^+$; C = Zn^{2+}, Fe^{2+}, Hg^{2+}, Cd^{2+}, Ni^{2+}, Mn^{2+}, Cu^{2+}, Cu$^+$ and Fe^{3+}; D = Sb^{3+}, As^{3+}, Bi^{3+} and Te^{4+}; Y = S^{2-} and Se^{2-}; and Z = S^{2-}, Se^{2-} and □ (Biagioni *et al.*, 2020a). Thus, tetrahedrite-group minerals are characterised by different homo- and heterovalent substitutions and represent an interesting link between mineralogy and ore geochemistry. The classification and nomenclature of the tetrahedrite-group minerals was published recently by Biagioni *et al.* (2020a). Silver-rich members with 3 to 6 Ag atoms per formula unit (apfu) (A-site constituent, freibergite/arsenofreibergite series) have been known for a long time. Indeed, 'freibergite' was first described from the Hab Acht Mine near Freiberg, Saxony, Germany by Weissenbach (1831) and named by Kenngott (1853). The Commission on New Minerals,

Nomenclature and Classification of the International Mineralogical Association (IMA–CNMNC) currently lists the freibergite series as argentotetrahedrite-(Fe) (Welch *et al.*, 2018), argentotetrahedrite-(Hg) (Wu *et al.*, 2021), argentotetrahedrite-(Zn) (Sejkora *et al.*, 2022), kenoargentotetrahedrite-(Fe) (the former freibergite – Welch *et al.*, 2018; Biagioni *et al.*, 2020a) and kenoargentotetrahedrite-(Zn) (Qu *et al.*, 2021). The arsenofreibergite series comprises fewer species, being currently populated only by argentotennantite-(Zn) (Spiridonov *et al.*, 1986; Biagioni *et al.*, 2020a) and kenoargentotennantite-(Fe) (Biagioni *et al.*, 2020b). The most common C-site constituent in minerals of the freibergite series is Fe (Riley, 1974; Pattrick and Hall, 1983; Peterson and Miller, 1986; Johnson *et al.*, 1986; Welch *et al.*, 2018; Biagioni *et al.*, 2020a) but some Cd-dominant chemical compositions have been reported previously (see a brief review below). Pattrick and Hall (1983) studied Ag substitution into synthetic Zn-, Cd-, and Fe-bearing tetrahedrites and for Cd members found the maximum Ag content of 7.02 apfu. The recent findings of a mineral specimen corresponding to argentotetrahedrite-(Cd) at the Rudno nad Hronom deposit, Slovak Republic, allowed the submission of a formal proposal to the IMA–CNMNC and the mineral and its name (symbol Attr-Cd) were approved (IMA2022-053, Mikuš *et al.*, 2022). Holotype material of argentotetrahedrite-(Cd) from Rudno nad Hronom is deposited in the collections of the Department of Mineralogy and

Petrology, National Museum in Prague, Cirkusová 1740, 19300 Praha 9, Czech Republic, under the catalogue number P1P 8/2022.

Occurrence and physical properties

Argentotetrahedrite-(Cd) was found at the Au–Ag epithermal deposit Rudno nad Hronom, Žarnovica Co., Banská Bystrica Region, Slovak Republic (48.396446°N, 18.682611°E) (Fig. 1).

The epithermal veins with Ag–Au mineralisation at this deposit are located in the western part of the Middle Miocene Štiavnica stratovolcano, represented mainly by andesitic rocks. The deposit is located in the southern and eastern slope of the Chlm hill extrusive complex over an area of 1.5 × 3 km. The mineralisation is situated in three large vein systems with a general S–N to NNW–SSE direction hosted in the first-stage andesitic complex of stratovolcano evolution related to a local horst structure (Lexa et al., 1999). Deeper parts of the mineralisation are developed in the basement rocks represented by sandstones, shales and Permian basalts of the Hronic unit (Smolka et al., 1988). The western flanks of the deposit host numerous swarms of granodiorite/quartz-diorite porphyry dykes (second stage of stratovolcano evolution) devoid of ore mineralisation. In the northern part of the deposit, a rhyolite dyke of the fifth stage of stratovolcano evolution penetrated the contact of the Chlm hill extrusive complex and the sills of andesite porphyry. According to Štohl et al. (1993), the mineralisation in Rudno nad Hronom area is genetically associated with the rhyolite volcanism of the fifth stage. The samples with argentotetrahedrite-(Cd) were collected from the Johan de Deo and Priečna vein accessible via the Johan de Deo adit. The ore shows a typical signature of low-sulfidation epithermal mineralisation with brecciated textures composed of fragments of the altered host rock, quartz, and disseminated precious and base-metal minerals. After the initial base-metal stage, the early precious metal stage of mineralisation starts by precipitation of argentotetrahedrite-(Zn) and tetrahedrite-(Zn) followed by greenockite together with argentotetrahedrite-(Cd) and 'tetrahedrite-(Cd)'. Argentotetrahedrite-(Cd) is replaced by later galena, acanthite, polybasite, pyrargyrite, bornite, stromeyerite, mckinstryite and Cu–S phases (chalcocite, digenite and covellite). Its crystallisation is related to the short activity of hydrothermal fluids rich in Cd (formation of greenockite and Cd members of the tetrahedrite group) during a precious metal stage of the formation of the Rudno nad Hronom Au–Ag epithermal deposit. The veins are located in hydrothermally altered rocks with abundant secondary K-feldspar, quartz, carbonates and smectites.

Argentotetrahedrite-(Cd) occurs as anhedral grains, up to 30 μm in size (Fig. 2), steel-grey in colour, tarnished to black and with a black streak. Lustre is metallic. The Mohs hardness may be close to 3½–4, as for other members of the tetrahedrite group. Argentotetrahedrite-(Cd) is brittle, with indistinct cleavage and conchoidal fracture. Density was not measured, owing to the small amount of available material; on the basis of the empirical formula and the single-crystal unit-cell parameters, the calculated density is 5.580 g/cm^3. In reflected light, argentotetrahedrite-(Cd) is isotropic. It is grey, with creamy tint and fast (tens of minutes) tarnishing to orange–brown. Internal reflections were not observed. Reflectance values, measured in air using a spectrophotometer MSP400 Tidas Leica microscope, with a 100× objective, are given in Table 1 and shown in Fig. 3, where they are compared with published data for argentotetrahedrite-(Zn) and argentotetrahedrite-(Fe).

Chemical data

Quantitative chemical analyses were carried-out using a Jeol JXA 8530 FE electron microprobe at the Geological Institute of Slovak Academy of Sciences, Banská Bystrica, Slovak Republic. Experimental conditions were: wavelength-dispersive spectroscopy mode, accelerating voltage 20 kV, beam current 15 nA and beam diameter 1 to 5 μm. Standards (element, emission line) were: pyrite (Fe$K\alpha$ and S$K\alpha$), chalcopyrite (Cu$K\alpha$), ZnS (Zn$K\alpha$), GaAs (As$L\beta$), Ag metal (Ag$L\alpha$), Sb$_2$S$_3$ (Sb$L\alpha$) and CdTe (Cd$L\alpha$). Peak counting times were 20 s for all elements, and 10 s for each background. Matrix correction by ZAF software was applied to the data. Due to possible vacancies at the S(2) site
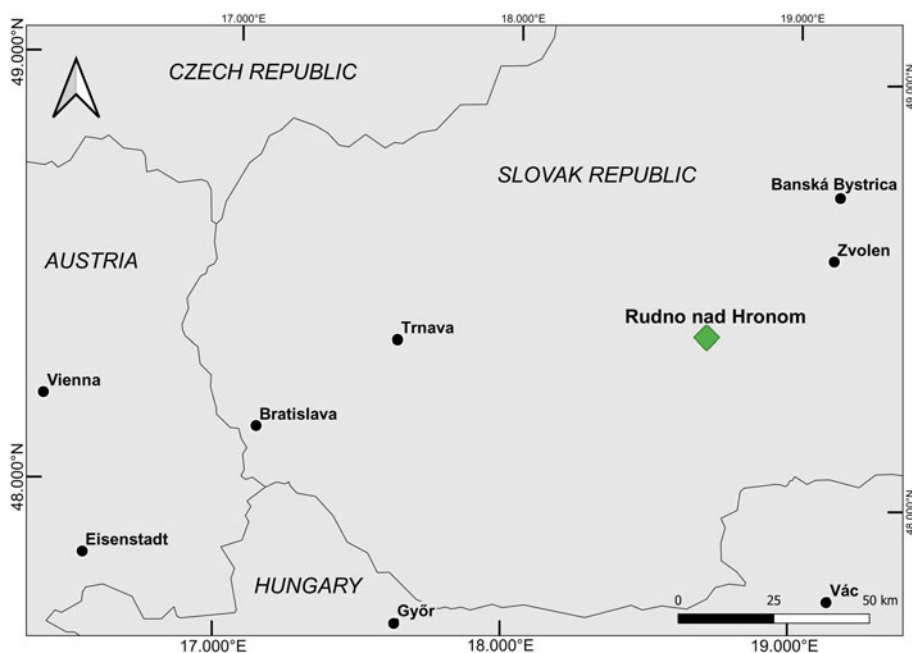

Fig. 1. Location of the Rudno nad Hronom, Banská Bystrica Region, Slovak Republic.
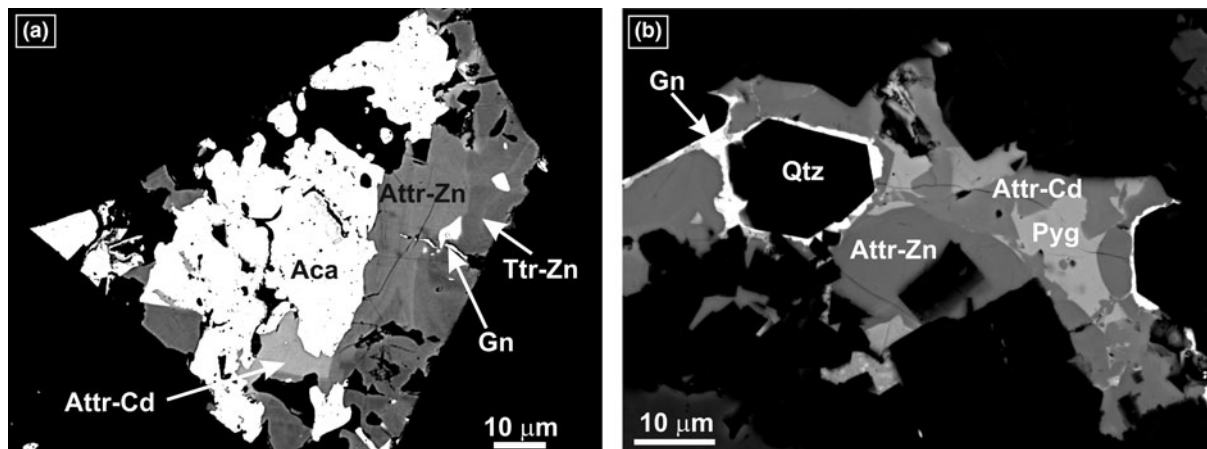
Fig. 2. (a) Argentotetrahedrite-(Zn) (Attr-Zn) and tetrahedrite-(Zn) (Ttr-Zn) associated with argentotetrahedrite-(Cd) (Attr-Cd) replaced by acanthite (Aca) and galena (Gn), Johan de Deo vein, Rudno nad Hronom, back-scattered electron (BSE) image (holotype, P1P 8/2022). (b) Argentotetrahedrite-(Cd) (Attr-Cd) associated with pyrargyrite (Pyg) are replacing argentotetrahedrite-(Zn) (Attr-Zn). The association is rimmed by younger galena (Gn), Priečna vein, Rudno nad Hronom, BSE image (specimen number is PR 0751). Symbols based on Warr (2021).

in the Ag-rich members, the chemical formula was calculated according to Biagioni *et al.*, (2020a) and Sejkora *et al.* (2021), where normalisation on the basis of $\Sigma Me = 16$ apfu, assuming that no vacancies occur at $M(2)$, $M(1)$ and $X(3)$ was used. The results of our study indicate that only very minor vacancies possibly occur at $M(2)$, $M(1)$ and $X(3)$ sites and therefore this approach was selected for calculation.

Chemical data for the argentotetrahedrite-(Cd) from Rudno nad Hronom (Table 2, Supplementary Table S1) give the formula $Cu_{6.74}Ag_{3.28}Cd_{1.68}Fe_{0.27}Zn_{0.16}(Sb_{3.71}As_{0.15})_{\Sigma3.86}S_{12.79}$. Taking into account the results of the crystal structure refinement (see below), the crystal-chemical formula can be written as $(Ag_{3.28}Cu_{2.72})_{\Sigma6.00}[Cu_4(Cd_{1.68}Fe_{0.27}Zn_{0.16})_{\Sigma2.11}]_{\Sigma6.11}(Sb_{3.71}As_{0.15})_{\Sigma3.86}S_{12.79}$. The end-member formula of argentotetrahedrite-(Cd) is $Ag_6(Cu_4Cd_2)Sb_4S_{13}$ ($Z = 2$), which requires (in wt.%) Ag 31.88, Cu 12.51, Cd 11.08, Sb 23.99, S 20.54, total 100.00.

The Ag content in the sample studied lies in the range 3.04–3.79 apfu and does not correlate with S (Fig. 4a). The positive correlation between Sb and Ag is indistinct (Fig. 4b), similarly as described for Ag-rich tetrahedrite by Johnson *et al.* (1986) and Sejkora *et al.* (2022). All samples studied have Cd as the dominant C-site constituent (Fig. 4c). Samples are mostly Fe-poor, with contents in the range of 0.08–0.49 apfu Fe. Moreover, the samples contain 0.04–0.30 apfu Zn. The extent of $SbAs_{-1}$ substitution is limited to 0.25 apfu As (Fig. 4d). The determined S contents in

the range 12.51–13.08 apfu indicates only minor possible vacancies at the S(2) site, consistent with the results of crystal structure refinement (see below).

Crystallographic data

Powder X-ray diffraction data could not be collected, owing to the small amount of the available material. Consequently, powder X-ray diffraction data, given in Table 3, were calculated through the software *Diamond v4.0* (from Crystal Impact, see Table 3) using the structural model of the sample from Rudno nad Hronom discussed below.

Slicing and polishing of lamellae for transmission electron microscope (TEM) analysis were carried out using a scanning electron microscope (SEM) coupled with a gallium-focused ion beam (FIB) source located at the Bauhaus University in Weimar, Germany. The SEM-FIB (Helios G4 UX, ThermoFisherScientific) is equipped with a high-performance FIB source (Phoenix) that allows polishing of TEM lamella at very low acceleration voltage or beam current. This feature is essential for obtaining undisturbed thin lamella suitable for high-resolution TEM imaging. Thin sections of samples as used for optical light microscopic investigation

Table 1. Reflectance data for argentotetrahedrite-(Cd) from Rudno nad Hronom.*

λ (nm)	R (%)	λ (nm)	R (%)
400	31.1	560	30.4
420	31.1	580	30.4
440	30.9	**589**	**30.3**
460	30.5	600	30.3
470	**30.4**	620	29.8
480	30.3	640	29.1
500	30.2	**650**	**28.7**
520	30.3	660	28.2
540	30.3	680	27.8
546	**30.3**	700	27.3

*The reference wavelengths required by the Commission on Ore Mineralogy (COM) are given in bold.
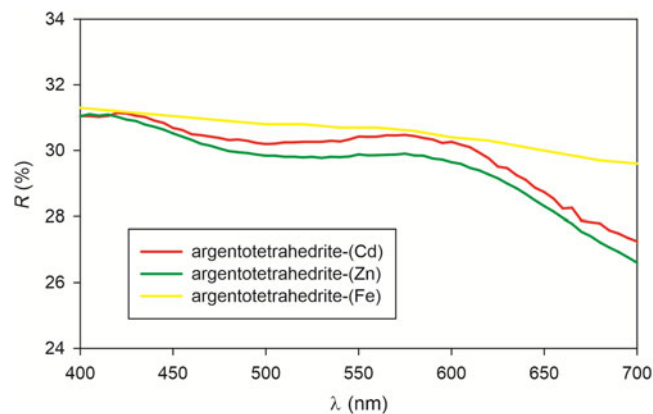

Fig. 3. Reflectance curves for argentotetrahedrite-(Cd) compared with data for argentotetrahedrite-(Zn) from Kremnica, Slovak Republic (Sejkora *et al.*, 2022) and argentotetrahedrite-(Fe) from Keno Hill, Yukon, Canada (Welch *et al.*, 2018).

Table 2. Chemical data for argentotetrahedrite-(Cd) (in wt.%, n = 14).

Constituent	Mean	Range	S.D. (σ)	Standard
Ag	18.92	17.68–21.47	0.41	Ag
Cu	22.92	21.75–23.76	0.27	$CuFeS_2$
As	0.62	0.14–0.98	0.32	GaAs
Sb	24.19	22.70–25.90	0.30	Sb_2S_3
Fe	0.80	0.18–1.60	0.28	FeS_2
Zn	0.56	0.15–1.50	0.45	ZnS
Cd	10.11	8.16–11.60	0.36	CdTe
S	21.95	21.55–22.90	0.49	FeS_2
Total	100.07	98.46–100.12	0.45	

S.D. – standard deviation

and other analyses were sputtered with ≈8 nm gold layer to ensure electric conductivity of the full sample and to reduce sample abrasion during ion-beam imaging. Sites for extraction of the lamellae were selected according to previous microscopic and spectroscopic characterisation of the samples. Areas of interest were covered with an approximately 15 μm × 15 μm × 3 μm layer of platinum as a further protection for the sample surface against ion beam damage.

The structure analysis was carried out at the ambient temperature using 3-dimensional electron diffraction (3DED) techniques. The 3DED data were collected on the lamella made from the argentotetrahedrite-(Cd) phase (Fig. 5a), with a continuous rotation mode in an FEI Tecnai 02 transmission electron microscope (TEM) (LaB_6 and acceleration voltage of 200 kV) equipped with a side-mounted hybrid single-electron detector ASI Cheetah M3, of 512 × 512 pixels with high sensitivity and fast readout (Institute of Physics, Czech Academy of Sciences, Prague, Czech Republic). A series of non-oriented patterns are continuously collected using a 0.5° step on all the accessible tilt range of the

goniometer (Gemmi and Lanza, 2019; Gemmi et al., 2019). The area of the lamella where data were collected is defined by the size of the 500 nm beam (nano-diffraction mode) (Fig. 5b). The data collection was automated by the in-house software, including the tracking of the crystal following the procedure described by Plana-Ruiz et al. (2020). Continuous-rotation 3DED data (cRED) reduction was performed using the computer program PETS2 (Palatinus et al., 2019; Klar et al., 2021). The specific data processing for cRED data used in the structure solution and the refinement is extensively detailed in Klar et al. (2021). It includes the introduction of overlapping virtual frames (OVF) for the dynamical refinement that aims to model experimental intensities from continuous rotation data by summing consecutive experimental diffraction patterns into a set of virtual frames. Each OVF is characterised by its angular range $\Delta\alpha_v$ covered by the virtual frame and the angular step between two virtual frames (see experimental details in Table 4).

The data reduction for the structure solution leads to an hkl-type file with R_{int}(obs/all) = 0.1532/0.1570 and 100% coverage for $\sin\theta/\lambda = 0.72$ $Å^{-1}$. For the dynamical refinement, another hkl-type file is generated where each OVF is considered independent in the refinement (Palatinus et al., 2015a, 2015b; Klar et al., 2021). The structure was solved using Superflip (Palatinus and Chapuis, 2007; Palatinus, 2013) in Jana2006 (Petříček et al., 2014) and refined using DYNGO and Jana2006.

Results and discussion

Crystal structure determination

The initial model obtained from the charge-flipping algorithm using Superflip, confirmed a tetrahedrite isotype structure with
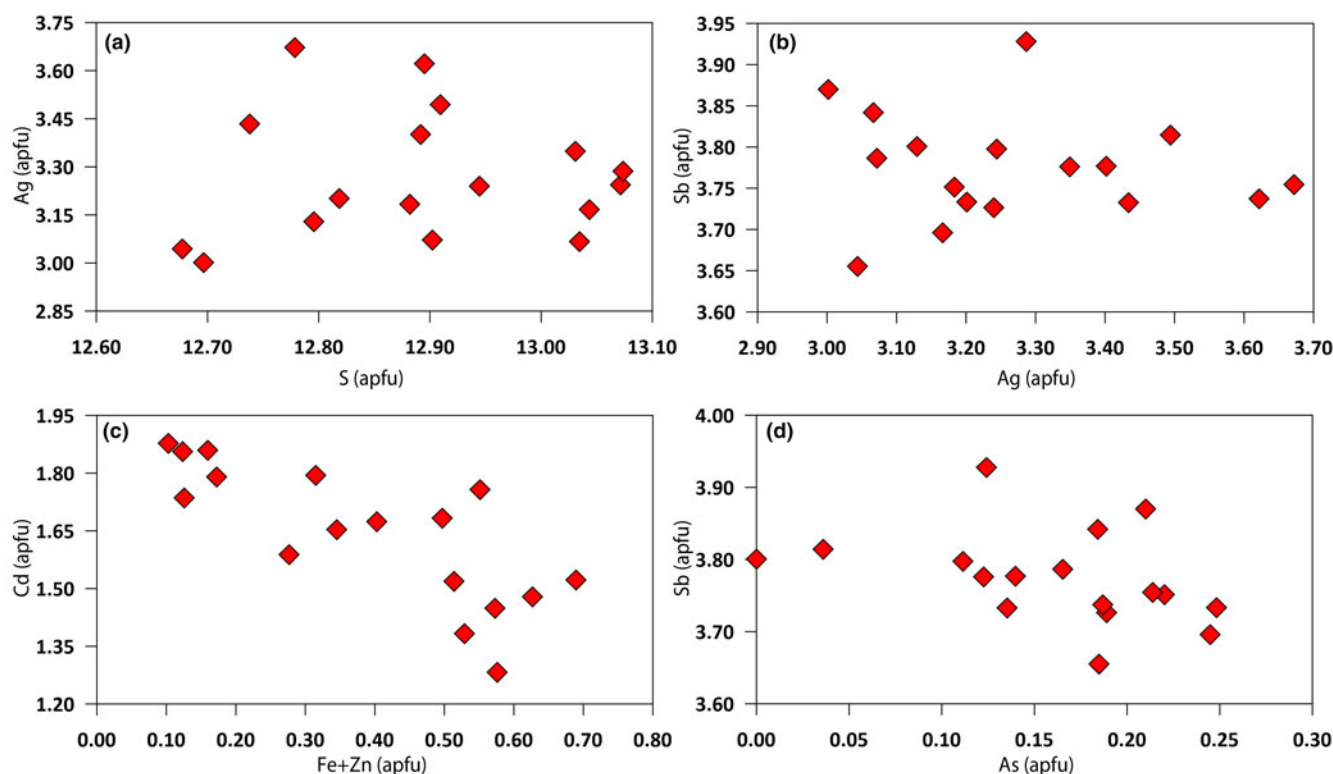

Fig. 4. Chemical relationships (in apfu) between Ag vs. S (a), Sb vs. Ag (b), Cd vs. Zn+Fe (c) and Sb vs. As (d) in argentotetrahedrite-(Cd) from Rudno nad Hronom.

Table 3. Calculated powder X-ray diffraction data for argentotetrahedrite-(Cd).*

I_{calc}	d_{calc} (Å)	hkl	I_{calc}	d_{calc} (Å)	hkl
3.7	7.5307	011	**5.9**	**1.9444**	**125**
2.3	4.3478	112	**48.1**	**1.8827**	**044**
3.6	3.7653	022	5.3	1.7277	116
100.0	**3.0744**	**222**	2.2	1.6433	145
5.6	**2.8463**	**123**	**30.3**	**1.6055**	**226**
26.3	**2.6625**	**004**	4.4	1.5372	444
6.1	**2.5102**	**114**	2.0	1.5061	055
4.3	2.2706	233	1.3	1.5061	345
4.4	2.0886	015	2.8	1.3526	237
4.8	2.0886	134	2.0	1.3526	156

* Calculated with *Diamond v4.0* (Diamond – Crystal and Molecular Structure Visualization, Crystal Impact – Dr. H. Putz & Dr. K. Brandenburg GbR, Kreuzherrenstr. 102, 53227 Bonn, Germany, https://www.crystalimpact.com/diamond). Intensity and d_{hkl} were calculated based on the structural model given in Table 5. Only reflections with $I_{calc} > 2$ are listed. The seven strongest reflections are given in bold.

three independent cation sites $M(1)$, $M(2)$ and $X(3)$ and two anion sites S(1) and S(2), in agreement with the general features of the tetrahedrite structure (Biagioni *et al.*, 2020a). Both sites S(1) and S(2) with Wyckoff positions 24g and 2a are attributed to S.

According to the electron microprobe (EMP) results, $X(3)$ (8c) is fully occupied by 96.1% of Sb^{3+} and 3.9% of As^{3+}. The substitution of Cu (Cu, Fe and Zn) by Ag and Cd in $M(1)$ (12d) and/or $M(2)$ (12e) was tested with dynamical refinement (see Table 5) using the composition from the chemical analysis. For well crystallised samples measured by 3DED, the best accuracy is reached when the dynamical effects (multiple scattering) are considered in the refinement (so-called 'dynamical refinement') (Palatinus *et al.*, 2015a, 2015b). Despite high quality data, the accuracy of the substitution tests remain limited as $M(2)$ tends to be disordered with a very high atomic displacement parameter value. The best compromise is found for the test in which Cd and Ag substitute for Cu in $M(1)$ and $M(2)$, respectively. After the last optimisations, the final refinement gives $R(obs)/wR(obs) =$

0.089/0.0891 and $R(all)/wR(all) = 0.1324/0.0943$ for 2316 observed reflections and only 14 outliers omitted following $|F_{obs}-F_{calc}|>15\sigma(F_{obs})$. No restriction was applied in the refinement. The structural parameters are presented in Table 6 and the interatomic distances in Table 7. The crystallographic information file has been deposited with the Principal Editor of *Mineralogical Magazine* and is available as Supplementary material (see below). The structure is represented with the atomic displacement parameters in Fig. 6a and the different sites in Fig. 6b.

The split option was tested from 3DED but it did not improve the model and the R factors were higher. The best compromise remained the non-split model. The accuracy limitation does not come from the 3DED data but the disorder that shadows a possible substitution by heavier atoms. X-ray data would show the same limitation in that case because none of those refinements (X-ray or 3DED) takes into account the inelastic scattering due to the disorder. The occupancies of the sites were constrained by the chemical results from the electron microprobe and varied to a degree that is reasonable for the data obtained. For this reason, the 3DED refined occupancy on the $M(2)$ is $(Ag_{0.55}Cu_{0.45})_6$; here we rely on the EMP analyses which gave a better idea of this occupancy as $Ag_{3.28}Cu_{2.72}$. (Table 2, 8). The sulfur sites appear to be fully occupied, thus providing no evidence for the existence of a $(Ag_6)^{4+}$ cluster. The EMP data indicate a small deficit on the anionic site, though, but not large enough to prove prevalence of the $(Ag_6)^{4+}$ clusters over the $(Ag_6^+S^{2-})^{4+}$ groups in the structure. Thus, combination of the electron-microprobe data and the structural model led to the classification of this mineral as argentotetrahedrite.

The determined unit-cell parameter for argentotetrahedrite-(Cd) from Rudno nad Hronom, $a = 10.65(2)$ Å, agrees very well with the value $a = 10.643$ Å calculated from our EMP data by relations proposed by Johnson *et al.* (1987) and is in line with parameters published for synthetic Cd–Sb dominant tetrahedrite by Patrick and Hall (1983): $a = 10.631$ Å (2.90 apfu Ag) and $a = 10.693$ Å (3.41 apfu Ag).
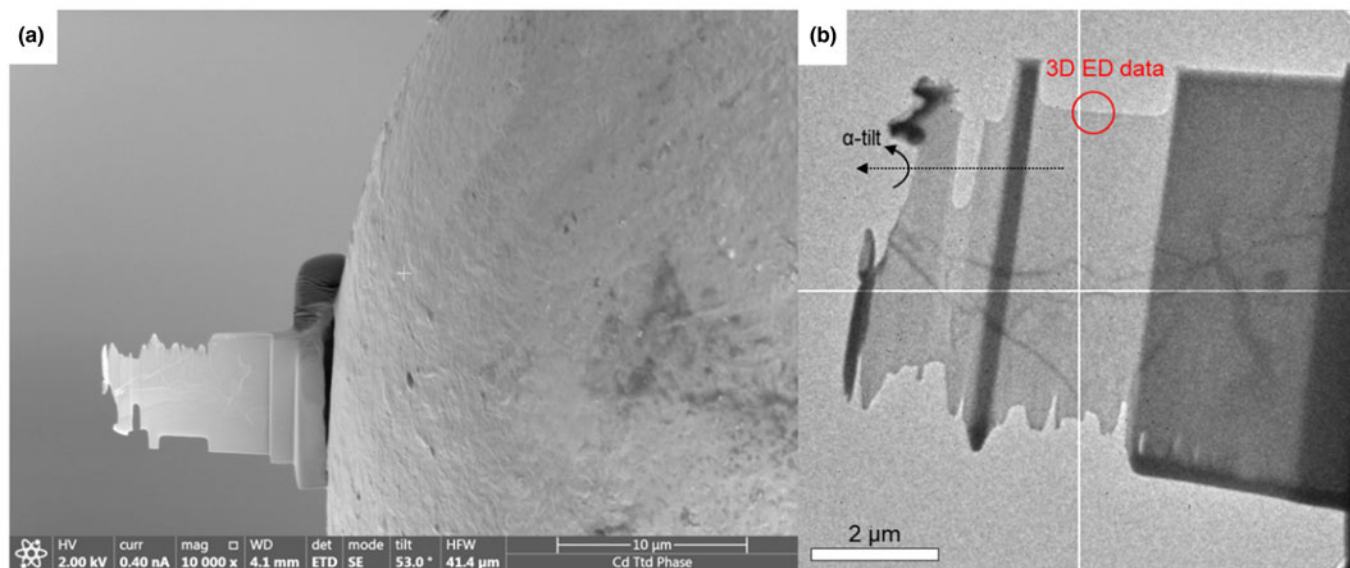

Fig. 5. (a) General view of the FIB lamella used for structure solution of argentotetrahedrite-(Cd). (b) Detail of the lamella, showing the region where the diffraction data were collected.

Table 4. cRED data collection and structure refinement details for argentotetrahedrite-(Cd).

Crystal data	
a (Å)	10.65(2)
V (Å^3)	1208(4)
Z	2
Density (g·cm^{-3})	5.1187
Space group	$I\bar{4}3m$
Data collection	
Temperature (K)	300
TEM	FEI Tecnai 02
Measurement method	Continuous rotation 3DED
Radiation (wavelength)	electrons (0.0251 Å)
$\Delta\alpha$/total α-tilt (°)	0.5/114
Resolution range (θ)	0.1–1.01
Limiting Miller indices	$-8 \leq h \leq 8,$
	$0 \leq k \leq 10,$
	$1 \leq l \leq 15$
No. of independent reflections (obs/all) – kinematic	318/367
R_{int} (obs/all) – kinematic	0.1532/0.1570
Redundancy	11.959
Coverage for $\sin\theta/\lambda = 0.7$Å^{-1}	100%
Dynamical refinement	
OVF: $\Delta\alpha_v$ /step between OVF (°)	4°/2°
Reflection selection criteria RSg(max)	0.6
Maximal diffraction vector g(max)	1.5 Å^{-1}
Number of integration steps	40
Filtered outliers $|F_{obs}-F_{calc}|>15\sigma(F_{obs})$	14
No. of reflections (obs/all)	2316/4572
R/ wR (obs); R/ wR (all)	0.089/0.0891; 0.1324/0.0943
No. refined param. all/structural	119/16
Effective thickness (Å)	196

Comparison between argentotetrahedrite-(Cd) and other members of the freibergite series

Argentotetrahedrite-(Cd) belongs to the freibergite series within the tetrahedrite group (Table 8) (Biagioni *et al.*, 2020a). It is the Cd-isotype of argentotetrahedrite-(Fe) (Welch *et al.*, 2018), argentotetrahedrite-(Zn) (Sejkora *et al.*, 2022) and argentotetrahedrite-(Hg) (Wu *et al.*, 2021).

Selected data for the argentotetrahedrite-(Cd) sample and valid (Zn/Fe/Hg)-members of the freibergite series are compared in Table 8. The Ag/(Ag + Cu) atomic ratio of 0.55 is similar to those in argentotetrahedrite-(Zn) (0.54) (Sejkora *et al.*, 2022). In the sample studied, the Sb/(Sb + As) ratio is >0.96. The increasing Cd/(Cd + Zn + Fe^{2+}) ratio also increases the unit-cell parameter, similarly as does increasing Hg^{2+} content (Table 8) because Cd^{2+} and Hg^{2+} have similar ionic radii (Johnson *et al.*, 1998). The $M(1)$–S(1) bond distance is not affected significantly by the Cd content. For argentotetrahedrite-(Fe) and -(Zn), the $M(1)$–S(1)

distance is 2.34 Å (Table 8). In argentotetrahedrite-(Cd), this distance is only slightly longer, 2.38 Å. In the $M(2)$ polyhedron, the $M(2)$–S(1) distance is definitely longer and more sensitive to the Ag content than the $M(2)$–S(2) distance, in agreement with previous studies (e.g. Peterson and Miller, 1986; Welch *et al.*, 2018, Sejkora *et al.*, 2022). Only few crystallographic data are available for the keno-members of the freibergite series. What is clear is that a detectable contraction of the unit-cell parameter can be observed for these keno-phases. For instance, kenoargentotetrahedrite-(Zn), having an Ag/(Ag + Cu) atomic ratio of 0.63, has a unit-cell parameter $a = 10.4624(4)$ Å (Qu *et al.*, 2021), significantly shorter than that given by Rozhdestvenskaya *et al.* (1993) for argentotetrahedrite-(Zn) with Ag/(Ag + Cu) = 0.60, i.e. $a = 10.576(3)$ Å. This difference probably reflects the contraction of the S(2)-centred $M(2)$-octahedron. In the two keno-members of the freibergite series, S ranges between 11.93 and 12.01 apfu, agreeing with the vacant nature of S(2). Indeed, the volume of the $M(2)$-octahedron is 10.8 Å^3 in kenoargentotetrahedrite-(Fe) (Welch *et al.*, 2018), to be compared with 16.2 Å^3 (+ 33%) in argentotetrahedrite-(Cd). This seems to be a clear structural feature allowing for the distinction between argentotetrahedrite and kenoargentotetrahedrite.

Previous findings of Cd-bearing tetrahedrite and tennantite: a brief review

The first Cd-member of the tetrahedrite group – tennantite-(Cd) was described recently by Biagioni *et al.* (2022). Tetrahedrite-group minerals having chemical compositions corresponding to that of argentotetrahedrite-(Cd) have been reported previously. To the best of our knowledge, the first chemical data corresponding to argentotetrahedrite-(Cd) were reported by Pattrick (1978), who gave microprobe analyses on samples from the Tyndrum, Perthshire, Scotland, showing 3.17 Ag apfu and 1.47 Cd apfu. In addition to this occurrence, other Cd-dominant members of the tetrahedrite series were reported from Xitieshan, Qinhai Province, China (Jia *et al.*, 1988) with Cd content 1.82 apfu and Evia Island, Greece (Voudouris *et al.*, 2011) with Cd up to 1.95 apfu. However, these tetrahedrite specimens do not belong to the freibergite series because their Ag content does not exceed 3 apfu. A phase similar to argentotetrahedrite-(Cd) was reported by Voropayev *et al.* (1988) from the Ushkatyn-III deposit in central Kazakhstan. Cadmium content varied between 0.93–0.99 apfu (recalculated on the basis of $\Sigma Me = 16$ apfu), Ag ≈ 3.1 apfu, and a Sb/(Sb + As) atomic ratio was 0.96. Dobbe (1992) reported microprobe data corresponding to composition varying between argentotetrahedrite-(Fe), 'argentotetrahedrite-(Mn)', and 'argentotetrahedrite-(Cd)'. Škácha *et al.* (2016) described

Table 5. Refinement tests (A–F) of the substitutions in $M(1)$ and $M(2)$ sites (without final optimisations or outlier filtering). Test C shows the best final statistics.

Test	A	B	C	D	E	F
U_{eq}(X(3))	0.02581	0.01945	0.01992	0.01879	0.02031	0.0197
$M(1)$	Cu	Cu/Ag	Cu/Cd	Cu/Ag/Cd	Cu	Cu/Ag/Cd
U_{eq}(M(1))	0.02488	0.05108	0.04164	0.0627	0.03125	0.04629
$M(2)$	Cu	Cu/Cd	Cu/Ag	Cu	Cu/Ag/Cd	Cu/Ag/Cd
U_{eq}(M(2))	0.05604	0.0721	0.089	0.05577	0.10933	0.08036
U_{eq}(S(1))	0.02402	0.02044	0.02304	0.01692	0.02545	0.02181
U_{eq}(S(2))	0.04741	0.04963	0.04373	0.05759	0.03691	0.04662
R(obs)	9.31	10.55	9.78	13.00	11.05	9.97
wR(all)	10.51	12.00	11.35	14.43	12.36	11.51

Table 6. Positional parameters and atomic displacement parameters.

Site, Wyckoff	Atom	s.o.f.	x	y	z	U_{eq} (Å²)	U^{11}	U^{22}	U^{33}	U^{12}	U^{13}	U^{23}
X(3), 8c	Sb1	0.9421	0.26748(7)	0.26748(7)	0.26748(7)	0.02016(18)	0.0202(3)	0.0202(3)	0.0202(3)	−0.0008(3)	−0.0008(3)	−0.0008(3)
X(3), 8c	As1	0.0578	0.26748(7)	0.26748(7)	0.26748(7)	0.02016(18)						
M(1), 12d	Cu1	¾	¼	½	0	0.0399(7)	0.0628(19)	0.0284(7)	0.0284(7)	0	0	0
M(1), 12d	Cd1	¼	¼	½	0	0.0399(7)						
M(2), 12e	Cu2	½	0.2158(2)	0	0	0.0851(8)	0.0649(17)	0.0952(12)	0.0952(12)	0	0	−0.0588(15)
M(2), 12e	Ag2	½	0.2158(2)	0	0	0.0851(8)						
S(1), 24g	S1	1	0.11790(17)	0.11790(17)	0.3631(2)	0.0216(5)	0.0210(7)	0.0210(7)	0.0227(13)	0.0041(9)	0.0037(7)	0.0037(7)
S(2), 2a	S2	1	0	0	0	0.0379(12)	0.038(2)	0.038(2)	0.038(2)	0	0	0

s.o.f. – site occupation factor.

Table 7. Interatomic distances (in Å).

X(3)–S(1)	2.472(6)	M(1)–S(1)ⁱⁱⁱ	2.384(6)	M(2)–S(1)ⁱ	2.370(6)
X(3)–S(1)ⁱ	2.472(6)	M(1)–S(1)ⁱᵛ	2.384(6)	M(2)–S(1)ᵛⁱ	2.370(6)
X(3)–S(1)ⁱⁱ	2.472(6)	M(1)–S(1)ⁱⁱ	2.384(6)		
		M(1)–S(1)ᵛ	2.384(6)	M(2)–S(2)	2.298(9)

Symmetry codes: [i] z, x, y; [ii] y, z, x; [iii] $-x + ½, -y + ½, z - ½$; [iv] $-x + ½, y + ½, -z + ½$; [v] $y, -z + 1, -x$; [vi] $z, -x, -y$; [vii] $-x + ½, -y + ½, z + ½$; [viii] $-x, -y, z$; [ix] $-y, z, -x$.
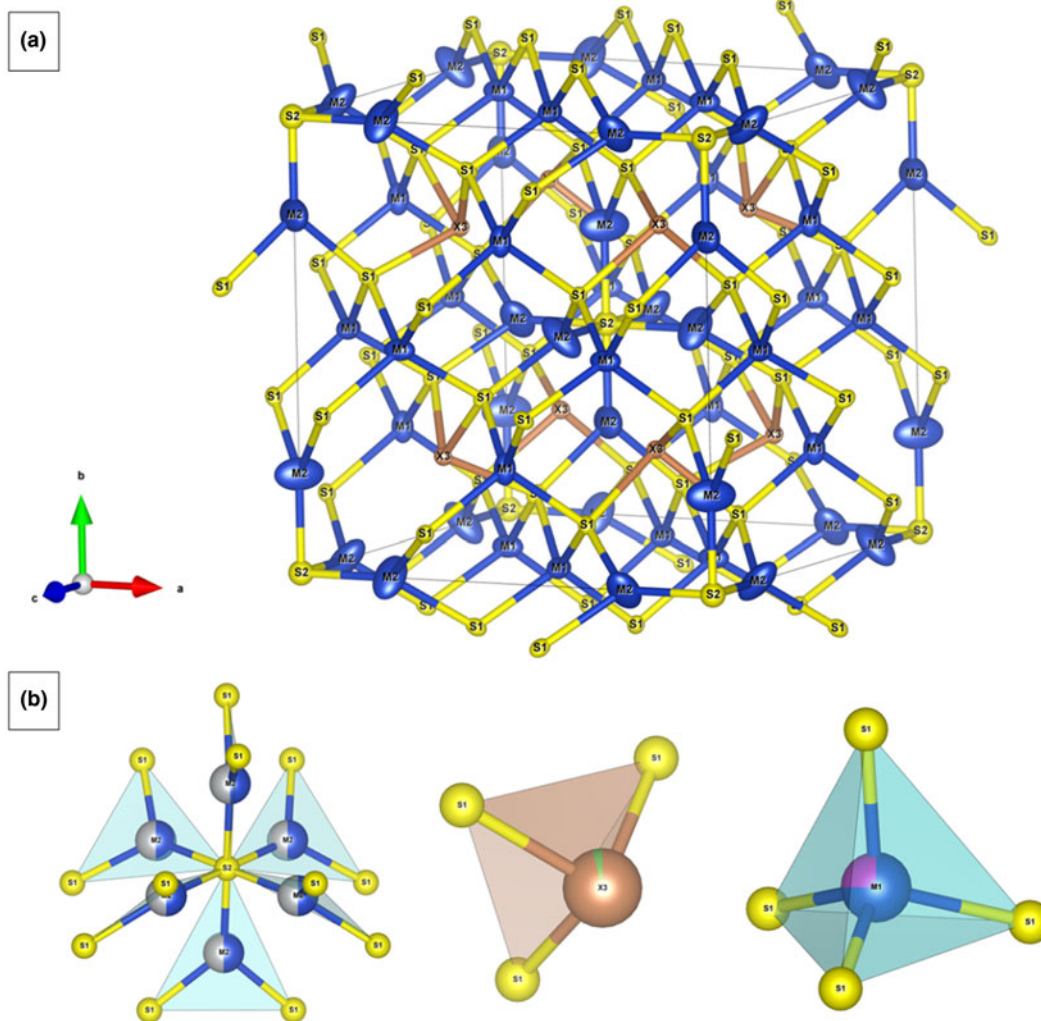
'Cd-hakite' [ideally $Cu_6(Cu_4Cd_2)Sb_4Se_{13}$] from Příbram in Czech Republic.

Synthetic analogues of Cd–Sb dominant tetrahedrite were studied by Pattrick and Hall (1983) who reported their unit-cell parameter $a = 10.631$ Å for a sample with 2.90 Ag apfu, and $a = 10.693$ Å for a sample with 3.41 apfu Ag.

Fig. 6. (a) The structure of argentotetrahedrite-(Cd) represented with anisotropic atomic displacement parameters. (b) The geometry of individual sites M(2), X(3) and M(1). Drawn using Vesta 3.0 (Momma and Izumi, 2020).

Table 8. Comparison of minerals of the argentotetrahedrite group*.

Site	Argentotetrahedrite-(Cd) This paper	Argentotetrahedrite-(Zn) Sejkora et al. (2022)	Argentotetrahedrite-(Fe) Welch et al. (2018)	Argentotetrahedrite-(Hg) Wu et al. (2021)
A_{ideal}	Ag	Ag	Ag	Ag
B_{ideal}	Cu	Cu	Cu	Cu
C_{ideal}	Cd	Zn	Fe	Hg
D_{ideal}	Sb	Sb	Sb	Sb
A_{meas}	$Ag_{3.28}Cu_{2.72}$	$Ag_{3.27}Cu_{2.69}$	$Ag_{4.37}Cu_{1.63}$	
B_{meas}	$Cu_{4.02}$	$Cu_{4.00}$	$Cu_{3.98}$	
C_{meas}	$Cd_{1.68}Fe_{0.27}Zn_{0.16}$	$Zn_{1.69}Fe_{0.23}Cu_{0.05}Cd_{0.02}Hg_{0.01}$	$Fe_{1.53}Zn_{0.40}$	
D_{meas}	$Sb_{3.71}As_{0.15}$	$Sb_{3.86}As_{0.17}$	$Sb_{3.86}As_{0.17}$	
$^{M(2)}$Ag/(Ag + Cu)	0.55	0.54	0.73	
$^{X(1)}$Sb/(Sb + As)	0.96	0.96	0.99	
Y + Z (apfu)	$S_{12.79}$	$S_{12.73}$	$S_{12.68}$	
a (Å)	10.65(2)	10.5505(10)	10.6116(1)	10.6511(2)
V (Å)	1208(4)	1174.4(3)	1194.92(2)	1208.3
M(2)–S(1) (Å)	2.370	2.386/2.464	2.437	
M(2)–S(2) (Å)	2.298	2.298/2.284	2.291	
M(1)–S(1) (Å)	2.384	2.339	2.344	

*The general structural formula of minerals belonging to the tetrahedrite group is: $^{M(2)}A_6{}^{M(1)}(B_4C_2)_{\Sigma 6}{}^{X(3)}D_4{}^{S(1)}Y_{12}{}^{S(2)}Z$ (Biagioni et al., 2020).

Conclusions

Following the approval of the new nomenclature of the tetrahedrite group (Biagioni *et al.*, 2020a), a renewed interest in this group of common sulfosalts has allowed for the definition of several new mineral species. Argentotetrahedrite-(Cd) is one of the latest additions to this group. In addition to the new mineral, new structural data have been collected, thereby improving our knowledge on the crystal chemistry of these chalcogenides.

Weathering of this mineral could release Cd into the environment and contaminate soil and water. Yet, the mineral is too rare, even at the type locality, to cause serious environmental damage. In addition, Cd has been shown to associate with CO_2 or carbonate ions in the environment (Lattanzi *et al.*, 1998, 2010). In samples like those studied in this work, abundant carbonates in the altered host rocks can buffer pH of the aqueous solutions in contact with the sulfides at relatively high values and supply the carbonate ions. Hence, the assemblage of Cd minerals in our samples (greenockite and argentotetrahedrite-(Cd)) is not expected to be of environmental concern.

Competing interests. The authors declare none.

References

Biagioni C., George L.G., Cook N.J., Makovicky E., Moëlo Y., Pasero M., Sejkora J., Stanley C.J., Welch M.D. and Bosi F. (2020a) The tetrahedrite group: Nomenclature and classification. *American Mineralogist*, **105**, 109–122.

Biagioni C., Sejkora J., Moëlo Y., Makovicky E., Pasero M. and Dolníček Z. (2020b) Kenoargentotennantite-(Fe), IMA 2020–062. In: CNMNC Newsletter 58. *Mineralogical Magazine*, **84**, 971–975.

Biagioni C., Kasatkin A., Sejkora J., Nestola F. and Škoda R. (2022) Tennantite-(Cd), $Cu_6(Cu_4Cd_2)As_4S_{13}$, from the Berenguela mining district, Bolivia: the first Cd-member of the tetrahedrite group. *Mineralogical Magazine*, **86**, 834–840.

Dobbe R.T.M. (1992) Manganoan-cadmian tetrahedrite from the Tunaberg Cu-Co deposit, Bergslagen, central Sweden. *Mineralogical Magazine*, **56**, 113–115.

Gemmi M. and Lanza A.E. (2019) 3D electron diffraction techniques. *Acta Crystallographica*, **B75**, 495–504.

Gemmi M., Mugnaioli E., Gorelik T.E., Kolb U., Palatinus L., Boullay P., Hovmoller S. and Abrahams J.P. (2019) 3D Electron Diffraction: The nanocrystallography revolution. *ACS Central Science*, **5**, 1315–1329.

Jia D., Fe Z., Zhang H. and Zhao C. (1988) The first discovery of Cd-freibergite in China. *Acta Mineralogica Sinica*, **8**, 136–137.

Johnson N.E., Craig J.R. and Rimstidt J.D. (1986) Compositional trends in tetrahedrite. *The Canadian Mineralogist*, **24**, 385–397.

Johnson N.E., Craig J.R. and Rimstidt J.D. (1987) Effect of substitutions on the cell dimensions of tetrahedrite. *The Canadian Mineralogist*, **25**, 237–244.

Johnson N.E., Craig J.R. and Rimstidt J.D. (1988) Crystal chemistry of tetrahedrite. *American Mineralogist*, **73**, 389–397.

Kenngott G.A. (1853) *Das Mohs'sche Mineralsystem, dem gegenwärtigen Standpuncte der Wissenschaft gemäss bearbeitet.* Gerold Verlag, Wien.

Klar P.B., Brazda P., Krysiak Y., Klementova M. and Palatinus L. (2021) Absolute configuration directly determined from 3D electron diffraction data. *Acta Crystallographica*, **A77**, C210.

Lattanzi P., Zuddas P. and Frau F. (1998) Otavite from Montevecchio, Sardinia, Italy. *Mineralogical Magazine*, **62**, 367–370.

Lattanzi P., Maurizio C., Meneghini C., Giudici G.D.E. and Podda F. (2010) Uptake of Cd in hydrozincite, $Zn_5(CO_3)_2(OH)_6$: evidence from X-ray absorption spectroscopy and anomalous X-ray diffraction. *European Journal of Mineralogy*, **22**, 557–564.

Lexa J., Štohl J. and Konečný V. (1999) The Banská Štiavnica ore district: relationship between metallogenetic processes and the geological evolution of a stratovolcano. *Mineralium Deposita*, **34**, 639–654.

Mikuš T., Majzlan J., Sejkora J., Vlasáč J., Steciuk G., Plášil J., Rößler C. and Matthes C. (2022) Argentotetrahedrite-(Cd), IMA 2022-053, in: CNMNC

Newsletter 69. *Mineralogical Magazine*, **86**, 988–992, https://doi.org/10.1180/mgm.2022.115.

Momma K. and Izumi F. (2020) VESTA 3 for three-dimensional visualization of crystal, volumetric and morphology data. *Journal of Applied Crystallography*, **44**, 1272–1276.

Palatinus L. (2013) The charge-flipping algorithm in crystallography. *Acta Crystallographica,* **B69**, 1–16.

Palatinus L. and Chapuis G. (2007) SUPERFLIP – a computer program for the solution of crystal structures by charge flipping in arbitrary dimensions. *Journal of Applied Crystallography*, **40**, 786–790.

Palatinus L., Petrícek V. and Corrêa C.A. (2015a) Structure refinement using precession electron diffraction tomography and dynamical diffraction: theory and implementation. *Acta Crystallographica*, **A71**, 235–244.

Palatinus L., Corrêa C.A., Steciuk G., Jacob D., Roussel P., Boullay P., Klementová M., Gemmi M., Kopeček J., Domeneghetti M.C., Cámara F. and Petříček V. (2015b) Structure refinement using precession electron diffraction tomography and dynamical diffraction: tests on experimental data. *Acta Crystallographica,* **B71**, 740–751.

Palatinus L., Brázda P., Jelínek M., Hrdá J., Steciuk G. and Klementová M. (2019) Specifics of the data processing of precession electron diffraction tomography data and their implementation in the program PETS2.0. *Acta Crystallographica*, **B75**, 512–522.

Pattrick R.A.D. (1978) Microprobe analyses of cadmium-rich tetrahedrites from Tyndrum, Perthshire, Scotland. *Mineralogical Magazine*, **42**, 286–288.

Pattrick R.A.D. and Hall A.J. (1983) Silver substitution into zinc, cadmium and iron tetrahedrites. *Mineralogical Magazine*, **47**, 441–451.

Peterson R.C. and Miller I. (1986) Crystal structure and cation distribution in freibergite and tetrahedrite. *Mineralogical Magazine*, **50**, 717–721.

Petříček V., Dušek M., and Palatinus L. (2014) Crystallographic Computing System Jana 2006: general features. *Zeitschrift Für Kristallographie—Crystalline Materials*, **229**, 345–352.

Plana-Ruiz S., Krysiak Y., Portillo J., Alig E., Estrade S., Peiro F. and Kolb U. (2020) Fast-ADT: A fast and automated electron diffraction tomography setup for structure determination and refinement. *Ultramicroscopy*, **211**, 112951.

Qu K., Sima X., Gu X., Sun W., Fan G., Hou Z., Ni P., Wang D., Yang Z. and Wang Y. (2021) Kenoargentotetrahedrite-(Zn), IMA 2020-075. CNMNC Newsletter 59. *Mineralogical Magazine*, **85**, 278–281, https://doi.org/10.1180/mgm.2021.5

Riley J.F. (1974) The tetrahedrite–freibergite series, with reference to the Mount Isa Pb–Zn–Ag orebody. *Mineralium Deposita*, **9**, 117–124.

Rozhdestvenskaya I.V., Zayakina N.V. and Samusikov V.P. (1993) Crystal structure features of minerals from a series of tetrahedrite-freibergite. *Mineralogiceskij Zhurnal*, **15**, 9–17 [in Russian].

Sejkora J., Biagioni C., Vrtiška L. and Moëlo Y. (2021) Zvěstovite-(Zn), $Ag_6(Ag_4Zn_2)As_4S_{13}$, a new tetrahedrite-group mineral from Zvěstov, Czech Republic. *Mineralogical Magazine*, **85**, 716–724.

Sejkora J., Biagioni C., Števko M., Raber T., Roth P. and Vrtiška L. (2022) Argentotetrahedrite-(Zn), $Ag_6(Cu_4Zn_2)Sb_4S_{13}$, a new member of the tetrahedrite group. *Mineralogical Magazine*, **86**, 319–330, https://doi.org/10.1180/mgm.2022.21

Škácha P., Sejkora J., Palatinus L., Makovicky E., Plášil J., Macek I. and Goliáš V. (2016) Hakite from Příbram, Czech Republic: compositional variability, crystal structure and the role in Se mineralization. *Mineralogical Magazine*, **80**, 1115–1128.

Smolka J., Skaviniak M., Valko P., Kámen M., Daubner J., Petr K., Gwerk E., Novák P., Kováč P., Ružiaková B. and Mjartanová, H. (1988) Final report of the project Rudno-Brehy-Pukanec. *Open File Report, Geological Survey of Slovak Republic, Bratislava*, 108 pp [in Slovak].

Spiridonov E.M., Sokolova N.G., Gapeev A.K., Dashevskaya D.M., Evstigneeva T.L., Chvileva T.N., Demidov V.G., Balashov E.P. and Shulga V.I. (1986) A new mineral – argentotennantite. *Doklady Akademii Nauk SSSR*, **290**, 206–210 [in Russian].

Štohl J., Lexa J., Kaličiak M. and Bacsó Z. (1993) Metallogenesis of base metal stockwork mineralisation in Western Carpathian Neogene volcanic rocks. *Open File Report, Geological Survey of Slovak Republic, Bratislava*, 87pp [in Slovak].

Voropayev V.K., Spiridonov E.M. and Shchibrik V.I. (1988) Cd-tetrahedrite, first find in the USSR. *Transactions of the USSR Academy of Sciences, Earth Science Sections*, **300**, 131–133.

Voudouris P.C., Spry P.G., Sakellaris G.A. and Mavrogonatos C. (2011) A cervelleite-like mineral and other Ag-Cu-Te-S minerals [Ag_2CuTeS and $(Ag,Cu)_2TeS$] in gold-bearing veins in metamorphic rocks of the Cycladic Blueschist Unit, Kallianou, Evia Island, Greece. *Mineralogy and Petrology*, **101**, 169–183.

Warr L. (2021) IMA–CNMNC approved mineral symbols. *Mineralogical Magazine*, **85**, 291–320, doi:10.1180/mgm.2021.43.

Weissenbach C.G.A. von (1831) Ueber die Gehalte der beym sächsischen Bergbau vorkommenden Silbererze. *Kalender für den Sächsischen Bergund Hüttenmann auf das Jahr 1831*, 223–248.

Welch M.D., Stanley C.J., Spratt J. and Mills S.J. (2018) Rozhdestvenskayaite $Ag_{10}Zn_2Sb_4S_{13}$ and argentotetrahedrite $Ag_6Cu_4(Fe^{2+}, Zn)_2Sb_4S_{13}$: two Ag-dominant members of the tetrahedrite group. *European Journal of Mineralogy*, **30**, 1163–1172.

Wu P., Gu X., Qu K., Yang H. and Wang Y. (2021) Argentotetrahedrite-(Hg), IMA 2020-079. In: CNMNC Newsletter 59. *Mineralogical Magazine*, **85**, 278–281.